U.S. DEPARTMENT OF ENERGY | Office of Science

DOE/SC-ARM-TR-330

Fixed-Site KAZR b1 Data Processing Report: 2025

M Rocque
M Deng
E Schuman
A Matthews

February 2026

ARM

DISCLAIMER

This report was prepared as an account of work sponsored by the U.S. Government. Neither the United States nor any agency thereof, nor any of their employees, makes any warranty, express or implied, or assumes any legal liability or responsibility for the accuracy, completeness, or usefulness of any information, apparatus, product, or process disclosed, or represents that its use would not infringe privately owned rights. Reference herein to any specific commercial product, process, or service by trade name, trademark, manufacturer, or otherwise, does not necessarily constitute or imply its endorsement, recommendation, or favoring by the U.S. Government or any agency thereof. The views and opinions of authors expressed herein do not necessarily state or reflect those of the U.S. Government or any agency thereof.

DOE/SC-ARM-TR-330

Fixed-Site KAZR b1 Data Processing Report: 2025

M Rocque
E Schuman
M Deng
A Matthews
All at Pacific Northwest National Laboratory

February 2026

How to cite this document:

Rocque, M, E Schuman, M Deng, and A Matthews. 2026. Fixed-Site KAZR b1 Data Processing Report: 2025. U.S. Department of Energy, Atmospheric Radiation Measurement User Facility, Richland, Washington. DOE/SC-ARM-TR-330.

Work supported by the U.S. Department of Energy,
Office of Science, Office of Biological and Environmental Research

Acronyms and Abbreviations

2D	two-dimensional
ARM	Atmospheric Radiation Measurement
ENA	Eastern North Atlantic
GE	general sensitivity
KAZR	Ka-band ARM Zenith Radar
KAZR2	second-generation Ka-band ARM Zenith Radar
KVNX	Vance Air Force Base NEXRAD radar
LDR	linear depolarization ratio
LPM	laser precipitation monitor
MD	moderate sensitivity
NEXRAD	Next-Generation Weather Radar
NSA	North Slope of Alaska
PLO	phase lock oscillator
PR	precipitation sensitivity
RF	radio frequency
SGP	Southern Great Plains
UTC	Coordinated Universal Time
VDIS	video disdrometer
VDISQUANTS	Video Disdrometer Value-Added Product

Contents

Figures

Tables

1.0 Introduction

The U.S. Department of Energy's Atmospheric Radiation Measurement (ARM) User Facility has been operating Ka-band ARM Zenith Radars (KAZRs) at each of its permanent observatories for at least the past 10 years. Data collected by the KAZRs is used to explore various cloud processes in different climatological regimes including marine stratocumulus clouds at the Eastern North Atlantic (ENA) site, arctic clouds at the North Slope of Alaska (NSA) site, and mid-latitude continental clouds at the Southern Great Plains (SGP) site.

The KAZRs operate in multiple modes that each have their own advantages and disadvantages. The general sensitivity (GE) mode provides data throughout the entire troposphere, including within 500 m of the surface, but is not as sensitive as the moderate sensitivity (MD) mode, which can observe weaker (smaller) signals. The MD mode does not collect data near the surface, though, and there can be additional artifacts in the data due to the processing. The second-generation KAZR (KAZR2) that operates at ENA has a third mode called precipitation sensitivity (PR) mode that is meant to be used in heavy precipitation when the other two modes are otherwise saturated by high returns. However, the PR mode transmits much lower than the GE and MD modes, which results in degraded sensitivity and should therefore only be used in heavy precipitation cases.

In 2025, ARM staff released five years (2020-2024) of corrected KAZR data from each of the fixed sites. These b-level data sets included corrections applied to the reflectivity for each mode and classification masks developed to filter out non-meteorological signals (Rocque et al. 2025). This report details the processing of b-level data for the fixed-site KAZRs for 2025 following the methods described in Rocque et al. (2025).

1.1 Radar Performance

The 2025 data availability for each fixed-site KAZR is shown in Figure 1. At ENA, the KAZR ran smoothly for most of the year. At NSA, there was about a month in August-September when the radar was offline while the antenna was replaced. At SGP, the radar was operational most of the year, but there was a nearly two-month period in June-July when the transmitter power was very low resulting in a significant degradation of the observed signals. The transmitter was replaced at the end of July, which restored the power output. However, starting in mid-August there have been concerns about the quality of the power moments due to a faulty phase lock oscillator (PLO). The impacts of this will be discussed in a later section.

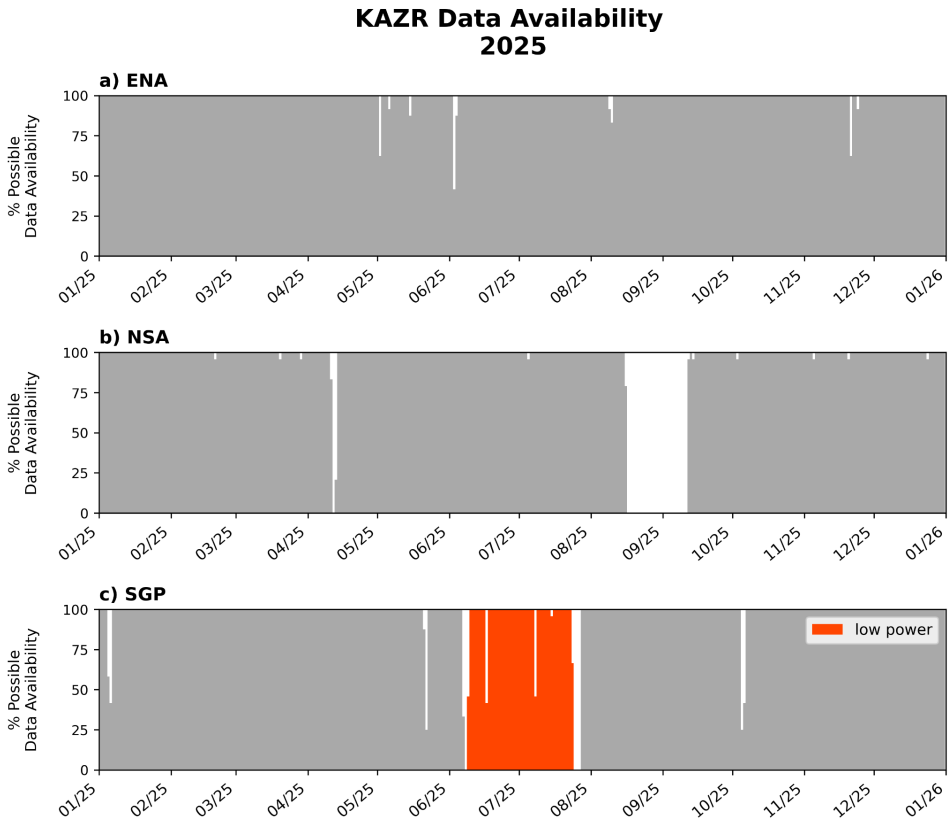

Figure 1. KAZR data availability at a) ENA, b) NSA, and c) SGP for 2025.

1.2 Outline for b1 Processing

The KAZR b-level processing involves estimating reflectivity offsets for each mode and creating masks that can be used to filter out non-meteorological signals and background noise. The following two sections describe the results of this process for KAZRs at ENA, NSA, and SGP for 2025. Additional details on the methodology can be found in Rocque et al. (2025).

2.0 Corrections

2.1 KAZR Intermode Comparison

Reflectivity from each of the KAZR modes is compared with one another to provide initial offsets. At ENA, there are two offset periods: before and after 2 May 2025. In early May, maintenance was performed on the KAZR2 to replace the drive amplifier. Before 2 May 2025, the difference between the GE and MD modes was around -2.4 dB while afterwards it was around -1.6 dB (Figure 2). The KAZR2 at ENA has a third mode (PR mode) that is also compared with the GE mode during 2025 (Figure 3). From 1 to 31 January 2025 the offset was quite significant with the PR mode about 14.1 dB lower than the GE mode. This is because the PR-mode radar constant does not account for changes in transmit power, and the initial transmit power used in the equation was from several years ago when it was much higher. The initial power was manually adjusted in the radar processing file on 31 January but was not correctly

applied until 6 February 2025. The offset during this week-long period was 7.6 dB and then starting 6 February 2025, the offset dropped to 0.5 dB. Two cases before (3 January 2025) and after (12 February 2025) this adjustment in the PR mode are shown in Figure 4. The PR-mode reflectivity agrees much better with the GE and MD modes after the adjustment to the calibration constant.

At NSA and SGP the reflectivity differences between GE and MD modes are stable across 2025, even with changes to the hardware (Figure 2). The NSA mean difference is -0.3 dB before and after the antenna replacement, and the SGP mean difference is 0.2 dB before and after the transmitter replacement.

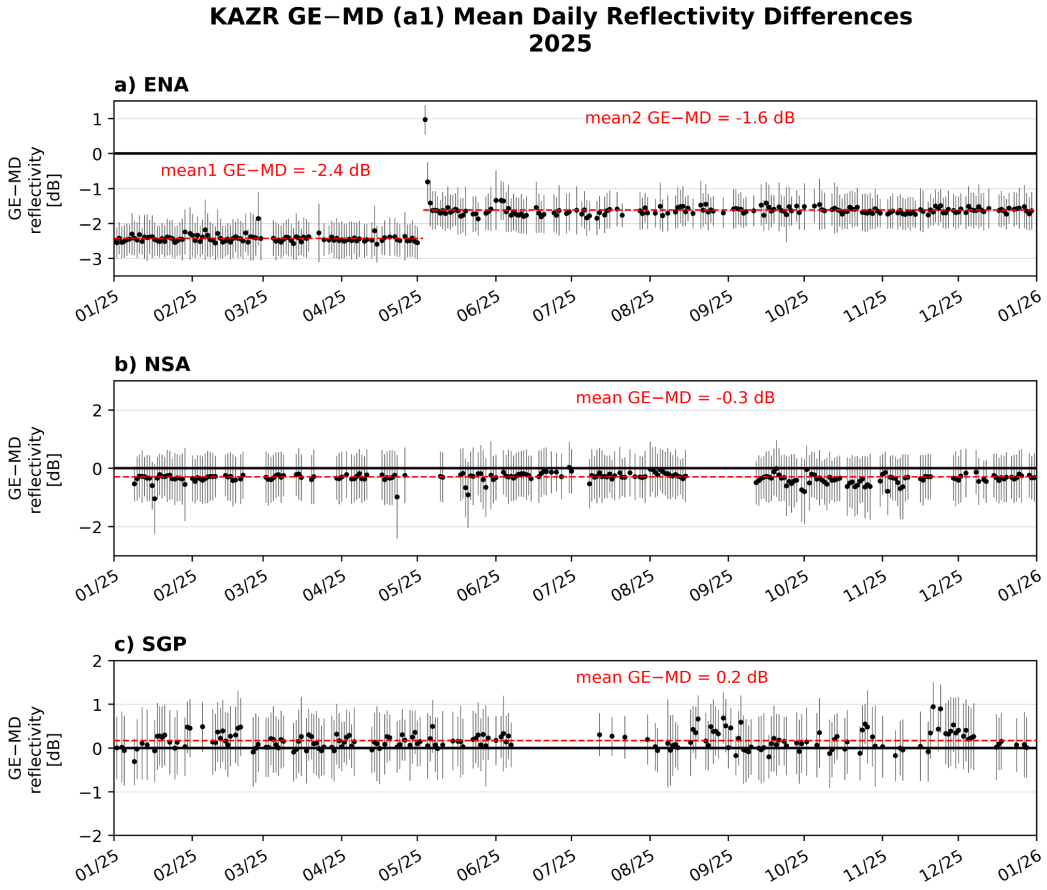

Figure 2. Time series of daily mean differences between KAZR a1 GE- and MD-mode reflectivity at a) ENA, b) NSA, and c) SGP for 2025. The means are shown in the red dashed lines and averages across each period are included on each subplot.

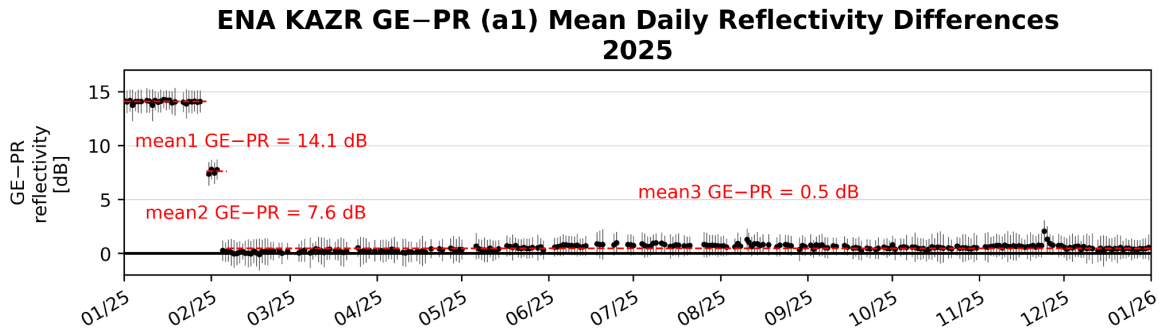

Figure 3. Time series of daily mean differences between ENA KAZR2 GE- and PR-mode reflectivity for 2025. There are three offset periods and the mean offset for each period is shown in the red dashed lines.

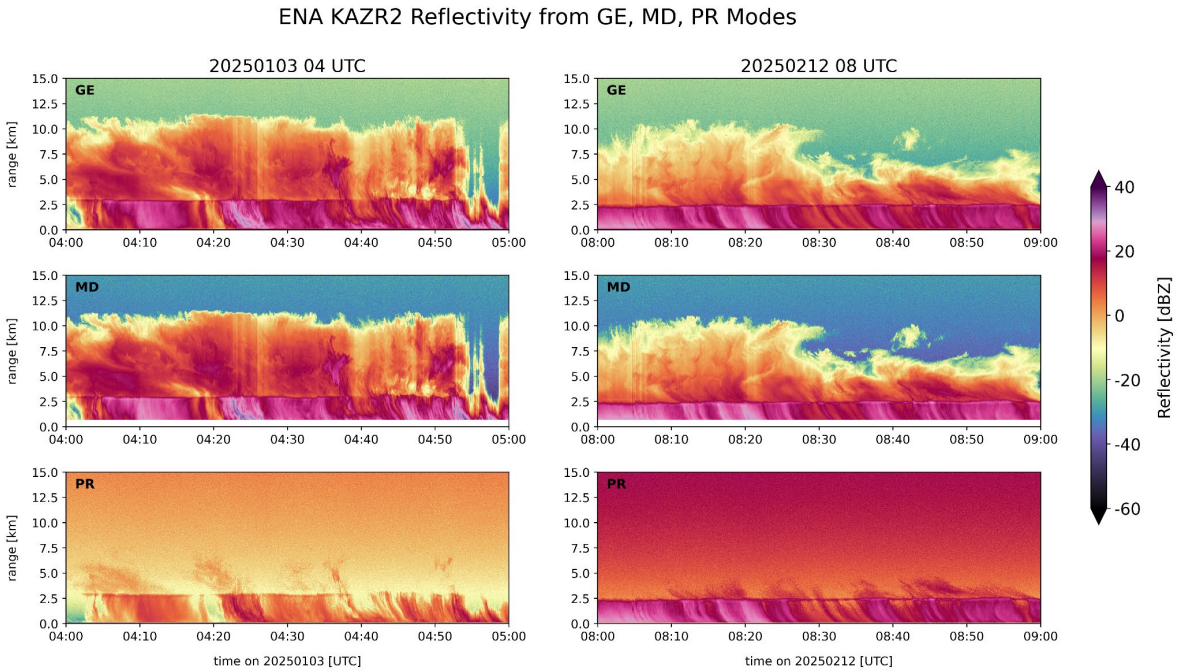

Figure 4. Time-height plots of reflectivity (dBZ) from the ENA KAZR2 GE (top), MD (middle), and PR (bottom) modes on (left) 3 January 2025 from 04-05 UTC (before the PR radar constant change) and (right) 12 February 2025 from 08-09 UTC (after the PR radar constant change).

2.2 KAZR Cross-Comparisons with Other Instruments

2.2.1 ENA KAZR versus VDIS

KAZR GE-mode reflectivity at 500 m is compared with surface-based disdrometer reflectivity estimated from the Video Disdrometer Value-Added Product (VDISQUANTS; Hardin et al. 2020). Before the comparison, a near-field correction and gaseous attenuation corrections are applied to the KAZR reflectivity (Sekelsky 2002, Ulaby et al. 1981). Once the comparison points have been identified, several additional thresholds are applied to filter out points that may be influenced by other factors such as

attenuation or non-meteorological signals that would otherwise impact the systematic bias. More details on the methodology and thresholds used can be found in the previous fixed-site KAZR b1 report (Rocque et al. 2025).

Histograms of ENA KAZR GE-mode reflectivity and video disdrometer (VDIS) reflectivity are shown in Figure 5. The VDIS tends to have more samples at lower reflectivities compared to the KAZR, but when filtering points between 5 and 15 dBZ, the offset between the two instruments is near 0 dB. Comparison points are then grouped by day to evaluate any potential trends in the offset. The time series shown in Figure 6 indicates the radar was stable throughout 2025, even after the maintenance performed in early May. The mean of the daily mean offsets from 2025 is also near 0 dB, suggesting the radar is well calibrated.

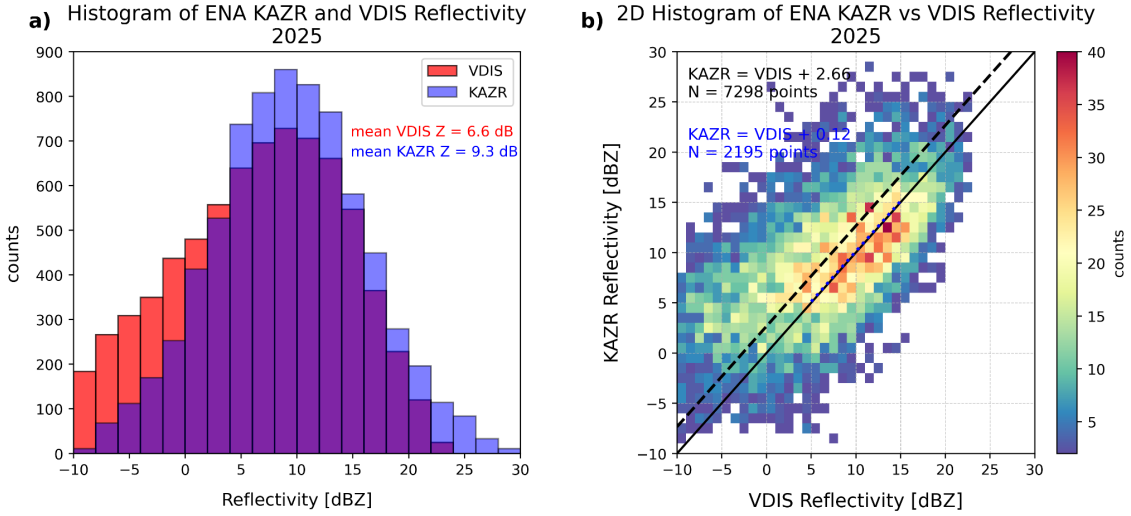

Figure 5. a) Histogram of Ka-band reflectivity from the ENA VDISQUANTS VAP (red) and the ENA KAZR GE mode (blue). The mean is shown in the upper left (6.6 dBZ for VDIS, 9.3 dBZ for KAZR). b) 2D histogram of ENA KAZR a1 GE-mode reflectivity versus Ka-band VDIS reflectivity with colors corresponding to the number of points within each bin. A one-to-one line is shown in solid black, a fitted line for all data points is shown in dashed black, and a fitted line for reflectivity between 5 and 15 dBZ is shown in dotted blue. The offsets for the fitted lines are shown in the upper left along with the total number of points. The mean offset between KAZR and VDIS is 0.1 dB when points are between 5 and 15 dBZ. The correlation between KAZR and VDIS reflectivity is 0.58.

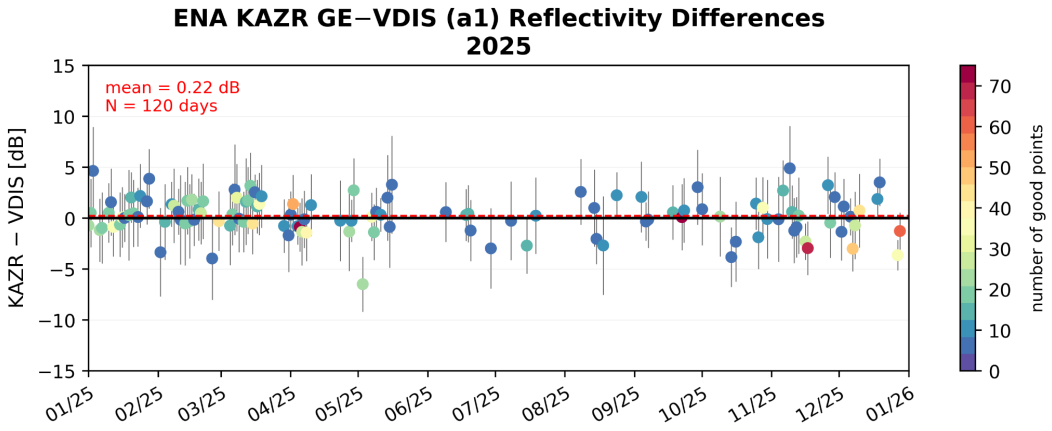

Figure 6. Time series of the daily mean differences between ENA KAZR a1 GE and VDIS reflectivity (dB). Each point is colored by the number of good points, and the error bars represent the standard deviation for that day. The mean of the daily mean differences is shown in the upper left (0.2 dB), and is plotted as the red dashed line. 120 days of data were used.

2.2.2 NSA KAZR versus LPM

A similar comparison is performed at the NSA site using the shielded laser precipitation monitor (LPM). Comparisons with the disdrometer are limited to liquid precipitation so only a small sample of days in 2025 are included in this analysis. As with ENA, the histogram analysis shows that the NSA KAZR is well calibrated in summer precipitation events compared to the LPM with the offset near 0.0 dB (Figure 7). While there were only 28 comparison days, the daily mean values are also generally around 0.0 dB, even after the antenna was replaced in August (Figure 8). Since there were no observed changes in the calibration constant or other radar parameters in the winter months, the radar is assumed to be well calibrated throughout 2025.

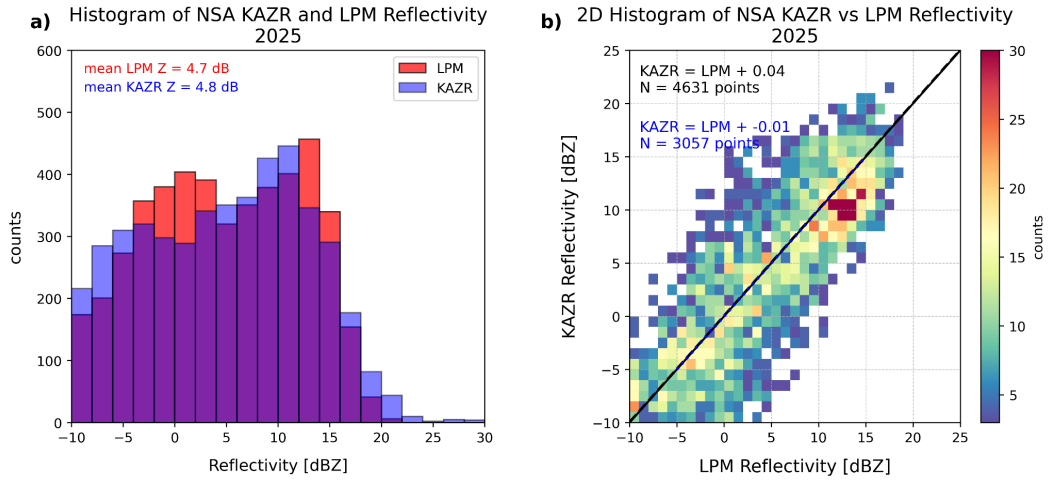

Figure 7. As in Figure 5 but for the NSA KAZR GE mode and the LPM. The mean offset between KAZR and LPM when points are between -5 and 15 dBZ is 0.0 dB. The correlation between KAZR and LPM reflectivity is 0.76.

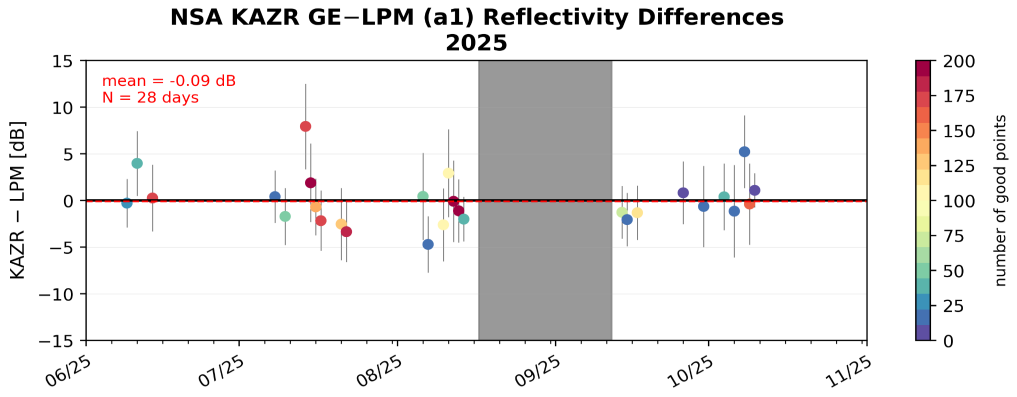

Figure 8. As in Figure 6 but for the NSA KAZR and the LPM. Only times when liquid precipitation was detected are plotted. The mean of the daily mean differences is about -0.1 dB and 28 days of data were used. The radar was not operating during the grey period (17 August-12 September 2025).

2.2.3 SGP KAZR versus KVNX

Due to the convective nature of events observed by the KAZR at SGP, hydrometeor and wet radome attenuation are often quite large, making comparisons with the disdrometer challenging. Thus, reflectivity offsets are estimated by comparing KAZR data with the KVNX (Vance Air Force Base) WSR-88D Next-Generation Weather Radar (NEXRAD) located about 60 km west of the site. Profiles of reflectivity are extracted from the KVNX scans over the KAZR and points are compared in non-precipitating ice clouds aloft. The results from 2025 show the KAZR reflectivity is about 3.5 dB lower than KVNX reflectivity (Figure 9). Plotting the daily mean differences between KAZR and KVNX reflectivity shows a slight shift beginning in mid-August (Figure 10). Before then, the offset is around 2.3 dB while afterwards it is around 4.7 dB. On 18 August 2025, the first significant jump in the linear depolarization ratio (LDR) was observed. These jumps continued throughout 2025 and have been attributed to a faulty PLO in the radio frequency (RF) unit. An example of these jumps in LDR is shown in Figure 11. When the histogram comparison is split before and after 18 August, there are clear differences that correspond well to the time series (Figure 12).

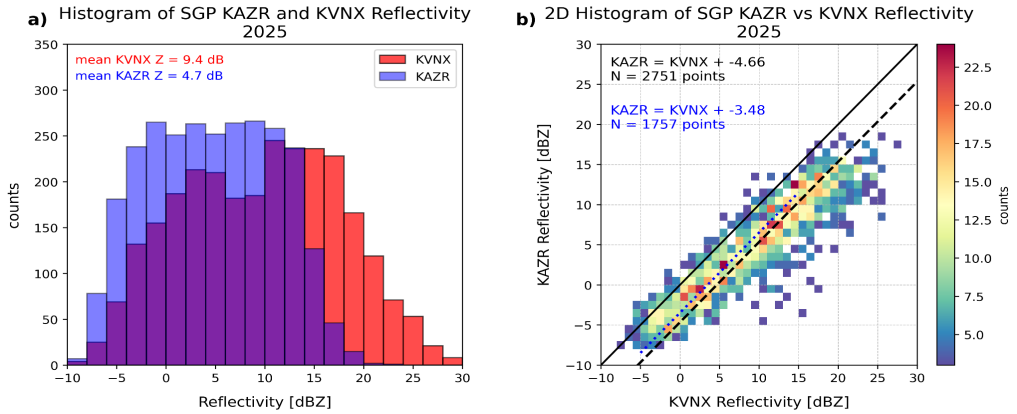

Figure 9. As in Figure 5 but for SGP KAZR GE mode and KVNX. The mean offset between KAZR and KVNX when points are between -5 and 15 dBZ is -3.5 dB. The correlation between KAZR and KVNX reflectivity is 0.85.

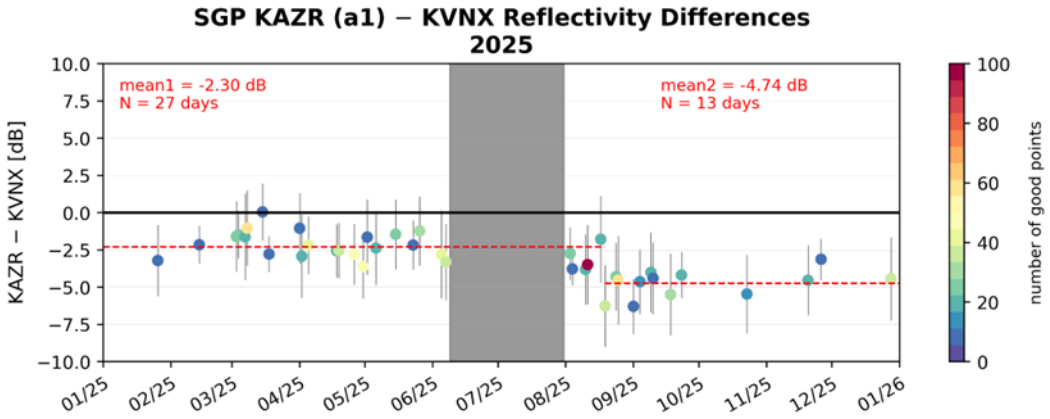

Figure 10. As in Figure 6 but for SGP KAZR GE mode and KVNX. The mean of the daily mean differences before 18 August 2025 is -2.3 dB and 27 days of data were used. The mean after 18 August 2025 is -4.7 dB and 13 additional days were analyzed. The radar transmitter was not working properly during the grey period (9 June-31 July 2025).

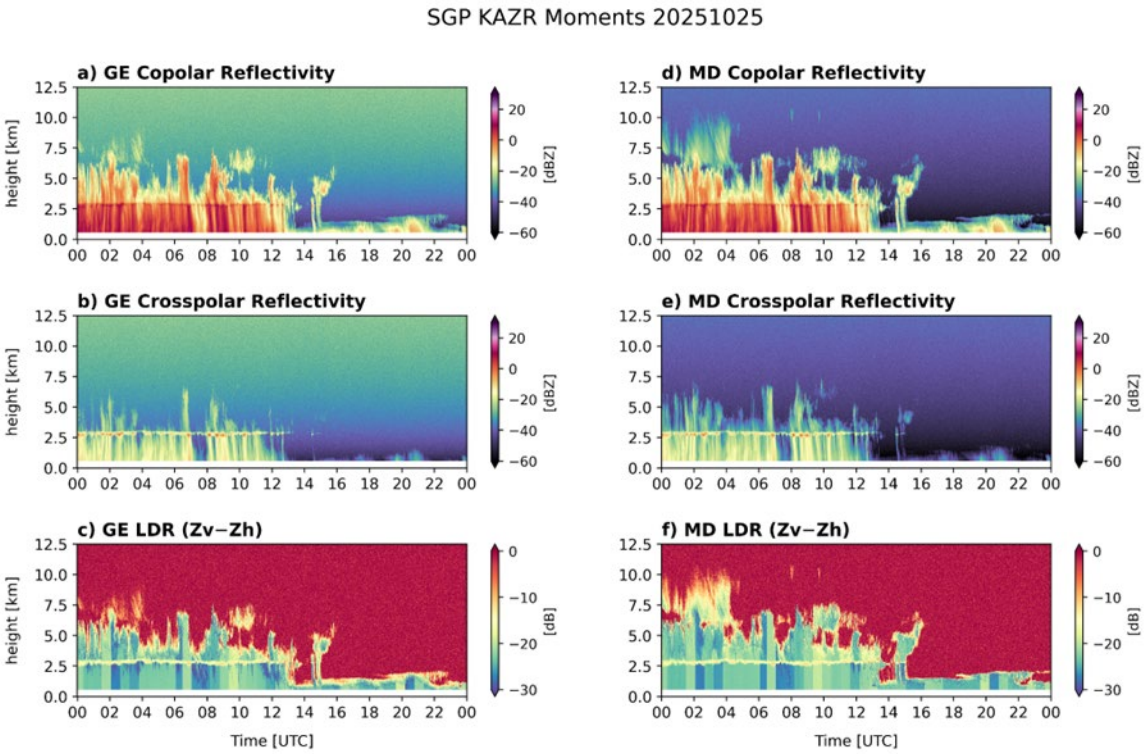

Figure 11. Time-height plots of co-polar reflectivity (dBZ; top), cross-polar reflectivity (dBZ; middle), and linear depolarization ratio (LDR; dB; bottom) from the SGP KAZR GE mode (left) and MD mode (right) on 25 October 2025.

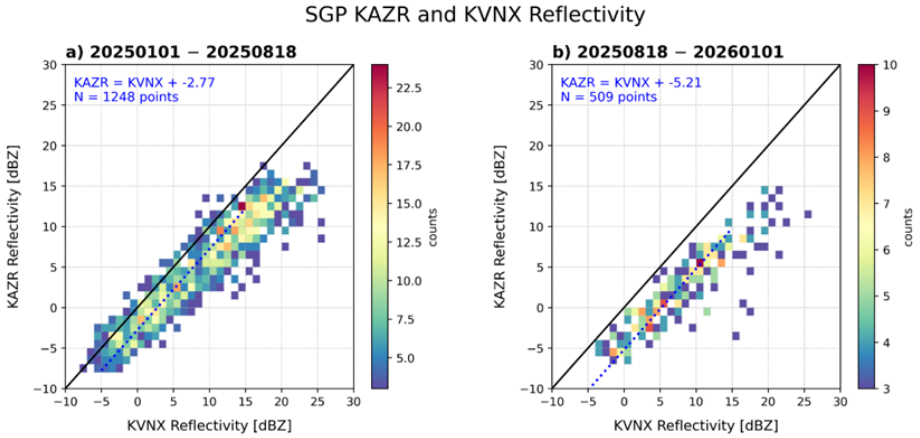

Figure 12. 2D histograms of SGP KAZR a1 GE-mode reflectivity versus KVNX reflectivity with colors corresponding to the number of points within each bin for a) 1 January to 18 August 2025 and b) 18 August through 31 December 2025. A one-to-one line is shown in solid black and a fitted line for reflectivity between -5 and 15 dBZ is shown in dotted blue. The offsets for the fitted lines are shown in the upper left along with the total number of points.

2.3 Summary of Reflectivity Offsets

A summary of the reflectivity offsets applied to the b-level fixed-site KAZR data for 2025 is shown in Table 1. At ENA, the disdrometer analysis showed the radar was well calibrated so no offset is applied to the GE mode. The MD-mode reflectivity offsets are determined from Figure 2 and suggest the reflectivity is slightly overestimated. The PR-mode reflectivity was significantly lower in January but only needs about 0.5 dB added back for the remainder of the year. At NSA, the summertime disdrometer analysis also showed the GE mode was well calibrated so there is similarly no offset applied here. The MD mode has a slight change of -0.3 dB throughout the year. At SGP, comparisons with KVNX showed the GE and MD modes were about 2.8 and 3.0 dB lower than expected before mid-August. The offsets became larger after the PLO began to malfunction, so 5.2 and 5.4 dB need to be added to the GE and MD modes, respectively.

Table 1. Reflectivity offsets (dB) applied to the b1 data during the indicated time frame for each KAZR mode.

Site, Mode	Time Frame	Offset Applied (dB)
ENA, GE	20250101 - 20260101	+0.0
ENA, MD	20250101 - 20250502	-2.4
	20250502 - 20260101	-1.6
ENA, PR	20250101 - 20250131	+14.1
	20250131 - 20250206	+7.6
	20250206 - 20260101	+0.5
NSA, GE	20250101 - 20260101	+0.0
NSA, MD	20250101 - 20260101	-0.3
SGP, GE	20250101 - 20250818	+2.8
	20250818 - 20260101	+5.2
SGP, MD	20250101 - 20250818	+3.0
	20250818 - 20260101	+5.4

3.0 Masks

The b-level KAZR data sets have two masks. The first is a basic censor mask that distinguishes background noise from signals using velocity texture. Areas with high velocity texture are background noise and can be removed using this mask. However, other non-meteorological signals such as insects and sidelobe artifacts in the MD mode are also considered signals with this basic mask. Therefore, a more advanced classification mask is developed to categorize these additional signals that may contaminate cloud analyses. The classification mask identifies background noise in addition to potential ground clutter, range sidelobes, which appear as false echoes above shallow cloud tops in the MD mode, and

biota (likely insects). This mask is not perfect but is meant to be used as a first pass to mask any non-meteorological echoes. Examples of the censor and classification masks applied at each site are shown in Figures 13-15.

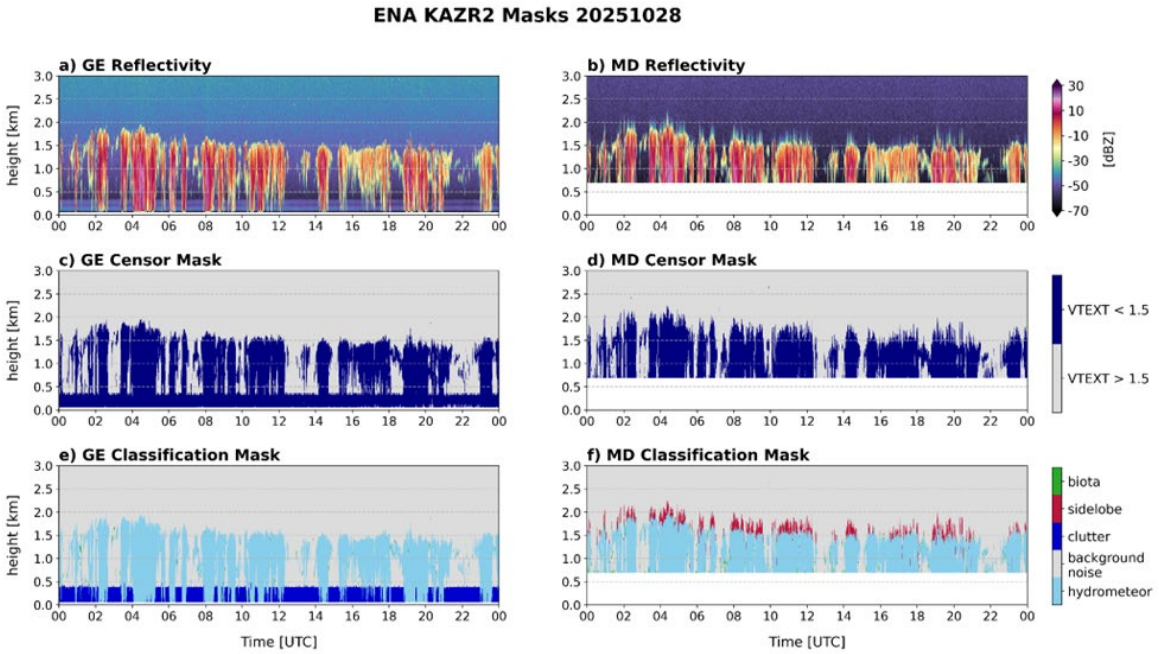

Figure 13. Time-height plots on 28 October 2025 of ENA KAZR2 a-b) reflectivity (dBZ), c-d) censor mask (velocity texture > 1.5 m s^{-1} = light grey; < 1.5 m s^{-1} = navy blue), and e-f) classification mask (hydrometeor = light blue; background noise = light grey; clutter = blue; sidelobe = red; biota = green) for GE mode (left) and MD mode (right).

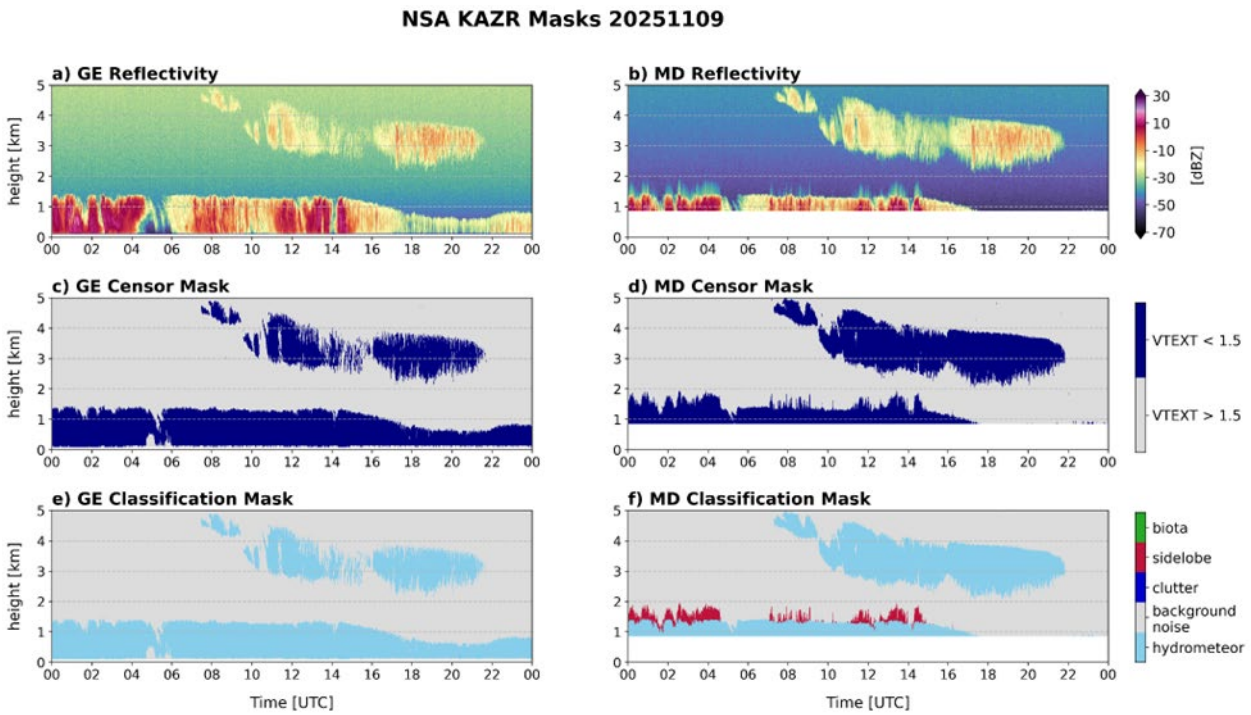

Figure 14. As in Figure 13 but for the NSA KAZR on 9 November 2025.

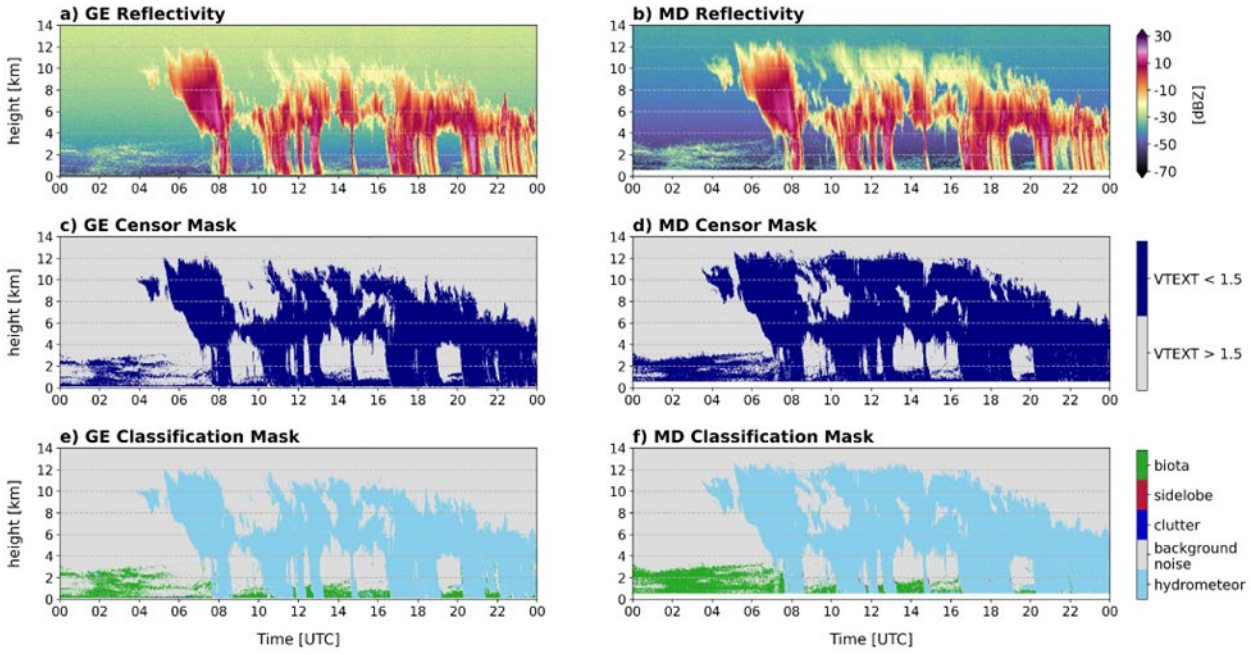

Figure 15. As in Figure 13 but for the SGP KAZR on 5 September 2025.

4.0 Description of Data Files

Some of the key variables in the b1-level radar datastreams for the KAZRs are listed below. The reflectivity field has corrections applied (Table 1), and the new mask detailed in Section 3 is included in the b1 data.

Key
Only in KAZR
Only in KAZR2
New variable calculated in b1 data
Correction applied

KAZR File Contents **(enakazr2cfrgeqcC1.b1, enakazr2cfrmdqcC1.b1, and enakazr2cfrprqcC1.b1)** **(nsakazrcfrgeqcC1.b1 and nsakazrcfrmdqcC1.b1)** **(sgpkazrcfrgeqcC1.b1 and sgpkazrcfrmdqcC1.b1)**	
Moments	
co_to_crosspol_correlation_coeff	copolar to cross-polar correlation coefficient (also known at rhoxh)
linear_depolarization_ratio	linear depolarization ratio, channel unspecified
mean_doppler_velocity	radial mean Doppler velocity, positive for motion away from the instrument
mean_doppler_velocity_crosspolar_v	Doppler velocity, cross-polar for vertical channel
reflectivity	equivalent reflectivity factor with offset applied
reflectivity_crosspolar_v	equivalent reflectivity factor, cross-polar for vertical channel
signal_to_noise_ratio_copolar_h	signal to noise ratio, horizontal channel
signal_to_noise_ratio_crosspolar_v	signal to noise ratio, cross-polar for vertical channel
spectral_width	spectral width
spectral_width_crosspolar_v	spectral width, cross-polar for vertical channel
Masks	
censor_mask	Bit mask 0: no mask 4: velocity_texture_above_threshold
classification_mask	Non-meteorological echo classification mask 0: hydrometeor 1: background noise 2: ground clutter 3: sidelobe 4: biota

5.0 References

Hardin, J, SE Giangrande, and A. Zhou. 2020. Laser Disdrometer Quantities (LDQUANTS) and Video Disdrometer Quantities (VDISQUANTS) Value-Added Products Report. U.S. Department of Energy, Atmospheric Radiation Measurement User Facility, Richland, Washington. DOE/SC-ARM-TR-221, https://doi.org/10.2172/1808573

Rocque, M, Y-C Feng, E Schuman, M Deng, A Matthews, and T Wendler. 2025. Fixed-Site KAZR b1 Data Processing: Corrections, Calibrations and Processing Report. U.S. Department of Energy, Atmospheric Radiation Measurement User Facility, Richland, Washington. DOE/SC-ARM-TR-320, https://doi.org/10.2172/2588592

Sekelsky, SM. 2002. "Near-field reflectivity and antenna boresight gain corrections for millimeter-wave atmospheric radars". *Journal of Atmospheric and Oceanic Technology* 19(4): 468–477, https://doi.org/10.1175/1520-0426(2002)019<0468:NFRAAB>2.0.CO;2

Ulaby, FT, RK Moore, and AK Fung. 1981. *Microwave Remote Sensing, Vol. I.* Addison-Wesley Publishing Company, Reading, Massachusetts.

www.arm.gov

U.S. DEPARTMENT OF
ENERGY

Office of Science